The Structure of 2-Oxo-4-hydroxy-4-carboxy-5-ureidoimidazoline Decarboxylase Provides Insights into the Mechanism of Uric Acid Degradation*[S]

Laura Cendron[‡§], **Rodolfo Berni**[¶], **Claudia Folli**[¶], **Ileana Ramazzina**[¶], **Riccardo Percudani**[¶1], and **Giuseppe Zanotti**[‡§2]

From the ‡Department of Chemistry, University of Padua, and Instituto di Chimica Biomolecolare-Consiglio Nazionale delle Ricerche, Section of Padua, Via Marzolo 1, 35131 Padua, Italy, ¶Department of Biochemistry and Molecular Biology, University of Parma, Viale delle Scienze 23/A, 43100 Parma, Italy, and §Venetian Institute of Molecular Medicine, Via Orus 2, 35127 Padua, Italy

The complete degradation of uric acid to (S)-allantoin, as recently elucidated, involves three enzymatic reactions. Inactivation by pseudogenization of the genes of the pathway occurred during hominoid evolution, resulting in a high concentration of urate in the blood and susceptibility to gout. Here, we describe the 1.8 Å resolution crystal structure of the homodimeric 2-oxo-4-hydroxy-4-carboxy-5-ureidoimidazoline decarboxylase, which catalyzes the last step in the urate degradation pathway, for both ligand-free enzyme and enzyme in complex with the substrate analogs (R)-allantoin and guanine. Each monomer comprises ten α-helices, grouped into two domains and assembled in a novel fold. The structure and the mutational analysis of the active site have allowed us to identify some residues that are essential for catalysis, among which His-67 and Glu-87 appear to play a particularly significant role. Glu-87 may facilitate the exit of the carboxylate group because of electrostatic repulsion that destabilizes the ground state of the substrate, whereas His-67 is likely to be involved in a protonation step leading to the stereoselective formation of the (S)-allantoin enantiomer as reaction product. The structural and functional characterization of 2-oxo-4-hydroxy-4-carboxy-5-ureidoimidazoline decarboxylase can provide useful information in view of the potential use of this enzyme in the enzymatic therapy of gout.

Uric acid, a key compound in the degradation pathway of purines (1), is degraded in many organisms to (S)-allantoin. It had long been thought that allantoin was formed directly from urate by the action of urate oxidase. However, a refined analysis of the urate oxidation reaction (2, 3) has led to the identification of other enzymatic activities associated with urate degradation (4, 5) and to the elucidation of the complete urate degradation pathway (6), involving three enzymatic reactions: oxidation of urate, catalyzed by urate oxidase, yields 5-hydroxyisourate (HIU),[3] which is then acted upon HIU hydrolase to yield 2-oxo-4-hydroxy-4-carboxy-5-ureidoimidazoline (OHCU); in turn, OHCU undergoes stereoselective decarboxylation by the action of OHCU decarboxylase to give CO_2 and (S)-allantoin (Scheme 1). In contrast, the slow non-enzymatic OHCU decarboxylation generates the racemic mixture of (S)- and (R)-allantoin (7).

Genes encoding for OHCU decarboxylase are present in a variety of organisms, including bacteria, fungi, plants, and metazoa and are tightly associated with urate oxidase and HIU hydrolase; in general, a species either has all three genes involved in urate degradation or none of them (6). Inactivation by pseudogenization of all three genes of the pathway occurred during hominoid evolution (6), resulting in high concentration of urate in the blood and susceptibility to gout. Urate oxidase is currently being employed therapeutically for refractory hyperuricemia (8). Addition of OHCU decarboxylase to this therapeutic regimen in humans could speed the conversion of urate oxidation products and thus make urate oxidase therapy better tolerated and safer.

The first enzyme of the pathway, urate oxidase, has been subjected to detailed structural characterization (9, 10). This enzyme is a multimer made up by four T-fold domains, a fold type that is found in other enzymes acting on purine or pterine substrates (11). The three-dimensional structure of HIU hydrolase has very recently been determined by four independent groups for bacterial (12–14) and vertebrate (15) organisms. HIU hydrolase is a homotetramer that structurally resembles a plasma transport protein, transthyretin; these two proteins represent a relevant example of divergent evolution. At variance with the two preceding enzymes of the pathway, OHCU decarboxylase, which has not been structurally characterized yet, has no similarity with other proteins. The structure of this enzyme was thus anticipated to reveal a novel fold and, possibly, a novel decarboxylation mechanism.

Here, we report on the crystal structure of OHCU decarboxylase from zebrafish and, based on the structures of the enzyme

---

The atomic coordinates and structure factors (code 2O7O, 2O73, and 2O74) have been deposited in the Protein Data Bank, Research Collaboratory for Structural Bioinformatics, Rutgers University, New Brunswick, NJ (http://www.rcsb.org/).

The nucleotide sequence(s) reported in this paper has been submitted to the DDBJ/GenBank™/EBI Data Bank with accession number(s) EF197726.

[S] The on-line version of this article (available at http://www.jbc.org) contains supplemental Fig. S1 and Table S1.

[1] To whom correspondence may be addressed. Tel.: 39-0521-905140; Fax: 39-0521-905151; E-mail: riccardo.percudani@unipr.it.

[2] To whom correspondence may be addressed. Tel.: 39-0498-275245; Fax: 39-0498-275239; E-mail: giuseppe.zanotti@unipd.it.

---

[3] The abbreviations used are: HIU, 5-hydroxyisourate; OHCU, 2-oxo-4-hydroxy-4-carboxy-5-ureidoimidazoline.

in complex with two different ligands and on mutational analysis of the enzyme active site, we provide insights into the mechanism and stereoselectivity of the enzymatic reaction.

EXPERIMENTAL PROCEDURES

Bacterial Expression and Purification of Wild-type and Mutant Forms of Zebrafish OHCU Decarboxylase and Mutational Analysis—The portion of the expressed sequence tag CN168729 (obtained from the Deutsches-Ressourcenzentrum für Genomforschung) encoding the complete sequence of zebrafish decarboxylase was PCR-amplified using a high fidelity thermostable DNA polymerase (Deep Vent DNA polymerase; New England Biolabs) and two sequence-specific primers: a NcoI-tailed upstream primer (5′-CCATGGATATAAATGTT-GTAAATGC-3′) and an EcoRI-tailed downstream primer (5′-GAATTCTTAGCTTCCCCTGTATG-3′). The amplification product digested with NcoI and EcoRI was cloned into the expression vector pET28b (Novagen). The expression of zebrafish decarboxylase in *Escherichia coli* BL21 (DE3) cells was induced by adding 1 mM isopropyl-1-thio-β-D-galactopyranoside; after a 4-h incubation at 28 °C, cells were lysed by 30-s bursts of sonication. The protein was purified to homogeneity using a one-step procedure consisting of gel filtration chromatography (Sephadex G100; Sigma) with a final yield of ~75

SCHEME 1. **Schematic representation of the pathway for enzymatic urate degradation.**

mg/liter of cell culture. Because the amino acid sequence of OHCU decarboxylase contains only 3 Met residues, one of which is at the N terminus, in order to solve the phase problem a mutant form with an additional Met residue was produced. The amino acid substitution L125M was selected on the basis of a multiple alignment of OHCU decarboxylase sequences showing the presence of a Met residue in position 125 in some piscine species (not shown). Mutant forms of OHCU decarboxylase (L125M, H67N, E87Q, and R161Q) were obtained by PCR using a high fidelity thermostable DNA polymerase (PfuUltra II Fusion HS DNA polymerase; Stratagene). The plasmid pET28b-OHCU decarboxylase was used as template, and mutagenic primers complementary to opposite strands were synthesized. The products of PCR were treated with DpnI (Stratagene) to digest the parental DNA template. This procedure allowed us to select the newly synthesized and potentially mutated plasmids. Single clones were then sequenced to confirm the occurrence of the desired mutation. Finally, mutant proteins were expressed and purified as described for the wild-type enzyme, with a final yield range of 35–90 mg/liter of cell culture. Se-Met-labeled enzyme was produced via inhibition of the Met metabolism pathway as described (16); cell cultures were induced with 1 mM isopropyl 1-thio-β-D-galactopyranoside and allowed to grow overnight at 25 °C. Se-Met-labeled enzyme was purified to homogeneity according to the procedure described above for wild-type OHCU decarboxylase. The oligomerization status of wild-type and mutant enzymes was verified by means of analytical gel filtration chromatography (Sephadex G100; Sigma). The enzymatic activities of purified wild-type and mutant forms of OHCU decarboxylase were evaluated as described, following the change of the OHCU-specific CD signal at 257 nm (6).

Crystallization, Data Collection, Structure Determination, and Refinement—Single crystals of the wild-type zebrafish OHCU decarboxylase (typical size: 0.15 × 0.1 × 0.1 mm) were obtained in 3–7 days, at 4 °C, by the sitting drop vapor diffusion method after equilibrating a solution containing OHCU decar-
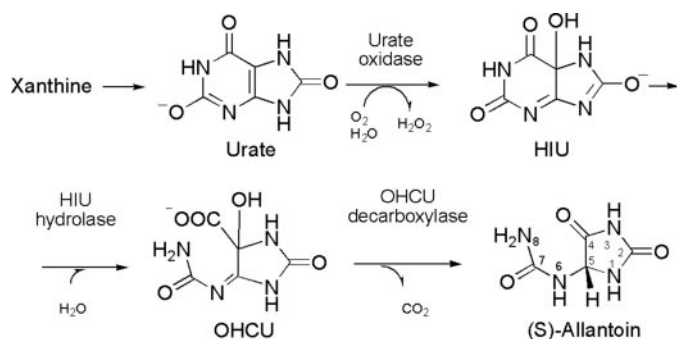
TABLE 1
Statistics on data processing and structure determination
Data in parentheses refer to the last resolution shell.

Data collections						
Data sets	Peak	Inflection point	Remote high	Native enzyme	Enzyme-(*R*)-allantoin complex	Enzyme-guanine complex
Wavelength (Å)	0.97878	0.97891	0.97604	1.07225		
Resolution range(Å)	103.69–2.50 (2.64–2.50)	104.83–2.60 (2.74–2.60)	103.69–2.50 (2.64–2.50)	67.12–1.80 (1.90–1.80)	88–1.80 (1.90–1.80)	86–1.80 (1.90–1.80)
Total reflections	456206 (55681)	143229 (19718)	315813 (39911)	568632 (79245)	279583 (24400)	653555 (56856)
Unique reflections	41687 (5888)	37561 (5494)	41787 (5966)	111211 (16284)	104588 (11935)	111719 (15859)
Multiplicity	10.9 (9.5)	3.8 (3.6)	7.6 (6.7)	5.1 (4.9)	2.7 (2.0)	5.8 (3.5)
R_{symm}	0.073 (0.362)	0.077 (0.383)	0.107 (0.331)	0.072 (0.409)	0.089 (0.449)	0.074 (0.438)
Mean $I/\sigma(I)$	26.0 (6.9)	14.4 (2.7)	18.0 (5.0)	17.4 (2.8)	9.5 (1.7)	5.7 (1.6)
Completeness (%)	99.5 (96.3)	99.7 (99.6)	99.5 (97.0)	99.9 (100.0)	93.0 (72.7)	99.6 (97.8)
Phasing statistics						
Phasing resolution (Å)	67.27-2.60	88.50-2.60	51.09-2.60			
Anomalous phasing power	2.072	0.904	0.700			
Figure of merit (acentric)	0.48770					
Refinement statistics						
Reflections(R_{free} set)				105633 (7466)	99340 (5361)	106440 (7583)
R_{cryst}				0.197 (0.267)	0.217 (0.338)	0.223 (0.317)
R_{free}				0.240 (0.345)	0.251 (0.338)	0.257 (0.385)
⟨B⟩ overall				22.5	23.0	24.0
⟨B⟩ for ligand				–	21.5	24.2
Root mean square deviation from ideal values						
Bond lengths (Å)				0.010	0.010	0.009
Bond angles (°)				1.16	1.20	1.18
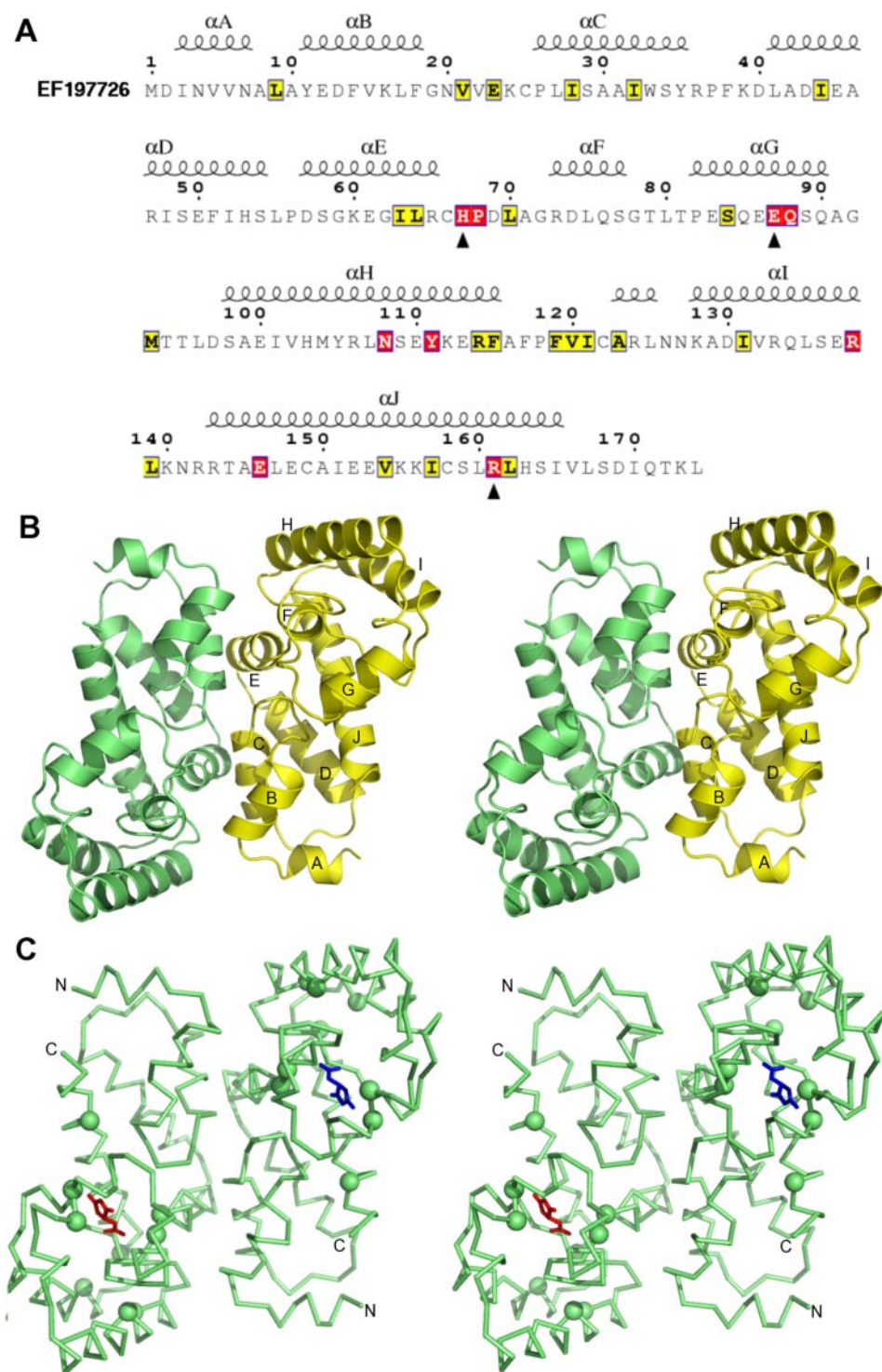
FIGURE 1. **Amino acid sequence and structure of OHCU decarboxylase.** *A*, amino acid sequence of zebrafish OHCU decarboxylase. Fully conserved or chemically similar residues in a multiple alignment of 60 protein sequences from different organisms are boxed in *red* and *yellow*, respectively (similarity groups: KR; DE; ST; NQ; AVLIM; FYW; P; G; C). *Upper line*, secondary structure elements based on definition of secondary structure assignments (DSSP) of the three-dimensional structure of OHCU decarboxylase (α-helices are labeled from *A* to *J*). The 3 residues involved in catalysis according to mutational analysis are marked with an *arrowhead* (see "Results and Discussion"). *B*, stereo view of the overall ribbon representation of dimeric OHCU decarboxylase. The view is roughly perpendicular to the molecular 2-fold axis; α-helices, defined as indicated in *panel A*, are labeled from *A* to *J*. *C*, stereo view of the Cα chain trace of the enzyme dimer with (*R*)-allantoin bound to the two active sites. Fully conserved residues are shown in space-filling representation. Labels *N* and *C* indicate N- and C terminus, respectively. *Panels B* and *C* were prepared by PyMOL (28).

boxylase (10 mg/ml), 10% (v/v) EtOH, 50 mM Tris-HCl, pH 8.5, against 20% (v/v) EtOH, 100 mM Tris-HCl, pH 8.5 (precipitant n.9 of Structure Screen 2; Molecular Dimension Ltd.). These crystallization conditions have been adopted for wild-type OHCU decarboxylase, the seleno-methionine derivative of the L125M enzyme mutant, and the wild-type enzyme in complex with guanine. Crystals of the enzyme in complex with allantoin were produced by soaking crystals of the wild-type enzyme with a racemic mixture of (*R*)- and (*S*)-allantoin for ~36 h. To obtain crystalline enzyme-ligand complexes, due to the poor solubility of guanine and allantoin an excess of these compounds from aqueous saturated solutions was added to the enzyme in solution prior to its crystallization or directly in the crystal, respectively. Data sets used for the determination of the structures described here were collected at cryogenic temperature (100 K) at beamlines ID23 and ID29 of European Synchrotron Radiation Facility (Grenoble, France). The best diffraction patterns were obtained with crystals soaked for ~30 s in a cryoprotectant solution containing 25% ethylene glycol, 20% EtOH, 100 mM Tris, pH 8.5. Crystals of both the native enzyme and Se-Met enzyme derivative belong to space group P3$_2$. Cell parameters for the native OHCU decarboxylase crystals are $a = b = 101.81$ Å, $c = 103.91$ Å; three dimers are present in the asymmetric unit, corresponding to a solvent content of ~50% and a V_M coefficient of 2.48 (17). A data set for the native enzyme was obtained at 1.8 Å resolution. A multiwavelength anomalous dispersion experiment was successfully performed using two crystals of the Se-Met enzyme derivative from the same crystallization drop. The best data sets collected with high redundancy around the selenium K edge showed an acceptable quality until 2.6 Å resolution. Data were processed with the programs MOSFLM and SCALA (18), and the corresponding

statistics are summarized in Table 1. The selenium substructure was identified by the program ShelxD (19). Interpretable maps were obtained by density modification and phase improvement procedures using the program AutoSHARP 2.2.0 (20). The rotation matrices and the translation vectors that relate the three dimers in the asymmetric unit were determined after the building of main chain atoms, with the help of the skeletonization procedure available in the Coot graphic software (21). Several cycles of model building and refinement applied to the high resolution data set for the native enzyme using both the packages CNS (22) and REFMAC (23) and incorporating non-crystallographic symmetry restraints allowed us to obtain a final overall crystallographic R factor of 0.199 (R_{free} 0.242). Residues 2–165 for all polypeptide chains A-F of the three dimers present in the asymmetric unit are clearly visible in the electron density map, with the exception of chain F, for which residues 1–168 are visible. The final model, analyzed with PROCHECK (24), is characterized by a good stereochemistry (no residues are present in disallowed or in generously allowed regions), with an overall G-factor of 0.2. Data sets for both complexes of the enzyme with either allantoin or guanine were obtained using one crystal each. Because the crystals of both complexes were found to be isomorphous with crystals of the native enzyme, refinement was carried out starting from the native enzyme refined structure. A Fourier difference map contoured at 3σ level clearly showed the presence of a ligand after the first cycles of refinement. The coordinates of the ligand, obtained with the server PRODRG (25), were introduced in the last cycles of refinement. In the case of allantoin, the electron density clearly reveals the presence of the (R) enantiomer. Individual B factors were refined in all models. The final statistics are detailed in Table 1. The search of structural homology for OHCU decarboxylase with deposited protein structures was performed with Profunc (26) and DALI (27).

RESULTS AND DISCUSSION

Overall Structure of OHCU Decarboxylase—OHCU decarboxylase is a homodimer in which the two polypeptide chains are related to each other by a molecular 2-fold axis. Each monomer, comprising 174 amino acids, is made up by ten α-helices (labeled *A* through *J*, Fig. 1, *A* and *B*) and is composed of two domains. The N-terminal domain (domain I) spans from residue Asp-2 to residue His-67 and includes the first five helices. The C-terminal domain (domain II) includes residues from Pro-68 to Ile-165 and the remaining five helices. The α-helices of domain I are rather short, between 5 and 10 residues long (α-helix C is quite irregular at its end, so that its length can be considered to span from 7 to 10 residues), with the exception of α-helix D, which comprises 14 residues. They are connected by short loops and fold up in a flat, compact domain. The segment 66–72, which is in extended conformation, connects domain I to domain II. The latter is formed by helices F through J: helix F (4 residues long) is the shortest, whereas helices H and J (18 and 22 residues long, respectively) are the longest. A long strand, mainly in extended conformation, is also present in this domain and connects helices H and I. The last helix, J, participates in the majority of contacts between the two
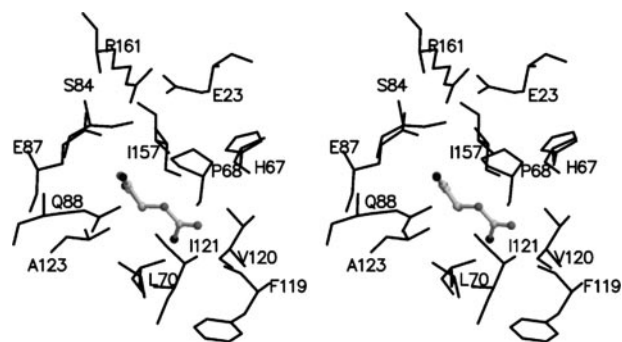

FIGURE 2. **Stereo view showing details of the active site of OHCU decarboxylase.** The C, N, and O atoms of bound (*R*)-allantoin (*ball-and-stick model*) are displayed as *light-gray*, *gray*, and *black spheres*, respectively.

domains. This arrangement confers to the monomer the shape of a flat parallelepiped, whose approximate size is $50 \times 35 \times 22$ Å (Fig. 1*B*). The amino acid sequence of OHCU decarboxylase (Fig. 1*A*) does not exhibit homology with other known amino acid sequences. Accordingly, in a search of structural homology with deposited protein structures, no significant structural similarity of other proteins with OHCU decarboxylase has been found. Therefore, a novel protein fold characterizes the structure described here.

21 potentially positively charged (Arg and Lys) and 25 negatively charged (Glu and Asp) residues are present in the model of the monomer (an additional Lys and an additional Asp are not visible in our model, being located in the C terminus). Most of these residues are on the surface of the molecule, with the exception of Glu-146, Arg-138 Glu-23, Arg-161, and Glu-87, whose charged side chains point toward the interior of the protein molecule, where they are involved in electrostatic interactions. Each monomer also contains 5 Cys residues that do not form disulfide bridges.

The dimeric state of the protein, which has been verified in solution by gel filtration (see "Experimental Procedures"), mainly involves interactions between α-helices C of one monomer and E of the other (and vice versa) and between the loop connecting helix B to helix C of both monomers. The area buried by dimerization is $\sim$2,300 Å^2/monomer. This large surface participates in both polar and apolar interactions, including 14 H-bonds (a list of the latter is reported in supplemental Table S1).

Structures of Allantoin- and Guanine-OHCU Decarboxylase Complexes and the Enzyme Active Site—Crystals of OHCU decarboxylase were soaked with a racemic mixture of (*S*)- and (*R*)-allantoin before data collection. A portion of the electron density of the Fourier difference map (supplemental Fig. S1) clearly shows that allantoin is bound inside a small cavity, the catalytic cleft, which is close to the external surface of the protein and is positioned between helix G and the stretches connecting helices H-I and E-F (Fig. 1*C*). It is located at the border of domain II of each monomer, in close contact with domain I, which partially lines its surface. Both hydrophilic and hydrophobic residues line the internal surface of the cavity (Fig. 2). The top of it, toward the solvent, is closed up by the side chains of Glu-87 and Arg-161. Glu-87 is neutralized by Arg-161; the latter also interacts with Glu-23,
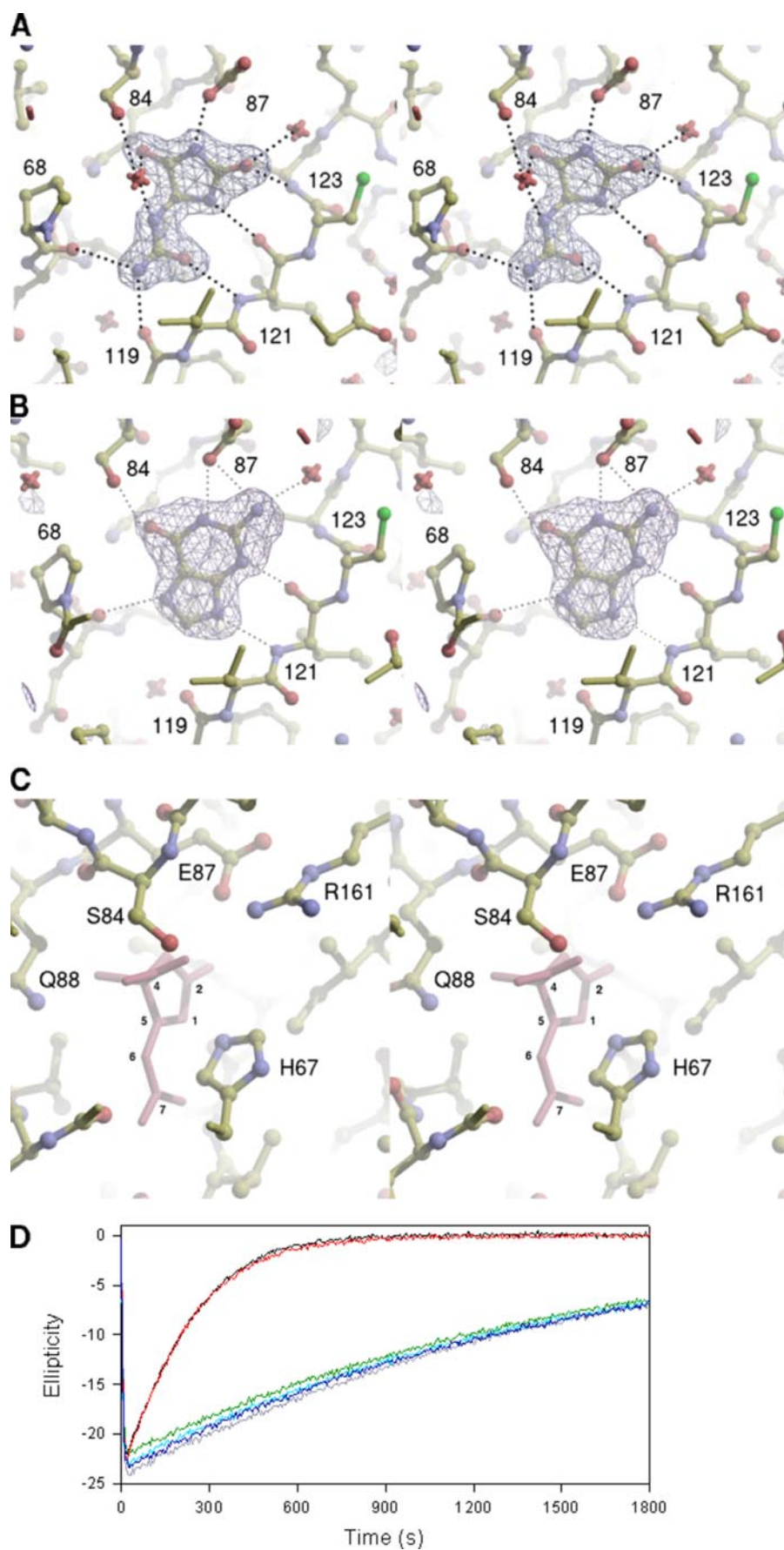
which in turn is neutralized by His-67. Therefore, an array of four alternating charges (Glu-87-Arg-161-Glu-23-His-67) is present at the enzyme active site. Other hydrophilic residues are Ser-84 and Gln-88. The side chains of residues Leu-70, Val-120, Ile-157, and Ala-123 form the hydrophobic portion of the cavity surface. Both active sites in the enzyme dimer are occupied by the ligand and are quite far apart, the distance between equivalent atoms of the two allantoin molecules being ~32 Å. The structural models of the liganded and unliganded states of OHCU decarboxylase are virtually identical (the root mean square deviation for the Cα atoms of the two dimers is in fact 0.1 Å), the space occupied by bound ligand being filled with five water molecules in the unliganded enzyme. Unexpectedly, (*R*)-allantoin, rather than the (*S*)-enantiomer, is found bound inside the cavity. Extensive interactions are established between (*R*)-allantoin and atoms of the enzyme active site (Fig. 3*A*). This pseudo-product of reaction participates in the formation of a number of H-bonds: all of the oxygen and nitrogen atoms of the ligand are at a distance shorter than 3.1 Å from protein N or O atoms or from a water molecule inside the active site. In particular, allantoin interacts with main chain atoms of residues 68, 119, 121, and 123, with the carboxylate group of Glu-87, and, through a water molecule, with the hydroxyl group of Ser-84 (Fig. 3*A*). The preferential binding of (*R*)-allantoin is consistent with the results of molecular modeling: in fact, by substituting this enantiomer with (*S*)-allantoin, some H-bond interactions are abolished. It should be noted that the residues mentioned above are conserved or chemically similar in the sequences of OHCU decarboxylases from phylogenetically distant species (Fig. 1*A*), consistent with their catalytic or conformational role at the enzyme active site.

Crystals of the enzyme in complex with guanine, a precursor of urate, were obtained by crystallization of the enzyme-ligand complex prepared in solution. The mode of binding of guanine is very similar to that of allantoin: nitrogen and oxygen atoms of the ligand make H-bonds with main chain atoms of residues 68, 119, 121, the carboxylate group of Glu-87, the hydroxyl group of Ser-84, and a water molecule (Fig. 3*B*). The superposition of bound allantoin and guanine shows that they occupy the same space inside the cavity but guanine is bound in a reverse way as compared with allantoin. The binding of each of the two enzyme ligands does not induce any conformational change in the protein. The active site cleft is a nearly closed cavity in both the liganded and unliganded states of the enzyme, so that we must assume that the protein undergoes transient conformational changes in order to provide access to OHCU and to permit the release of allantoin from the active site. Movements of the side chains of Glu-87 and Arg-124, and possibly of residues Ala-123 and Leu-125, are likely to take place to allow substrate binding and product release.

Putative Catalytic Mechanism—A modeling of enzyme-bound OHCU in the position occupied by allantoin in the crystal structure (Fig. 3*C*) indicates that the carboxylate group of Glu-87 is close to the carboxylate of the substrate: the distance between oxygen atoms of the two negatively charged groups is ~3 Å, possibly causing an electrostatic repulsion between them. In the crystal structure of the allantoin-OHCU decarboxylase complex, the imidazole ring of His-67 is at a distance of ~5.5 Å from the C5 atom of the five-membered ring of the substrate, but a simple rotation around the Cα-Cβ bond of His-67 can reduce this distance to ~3 Å, or even less (Fig. 3*C*). This model suggests that at least 2 residues, Glu-87 and His-67, are close to the substrate and in a position suitable for playing a crucial role in catalysis. Besides, the enzymatic reaction could be indirectly affected by Arg-161 and Glu-23, the other 2 charged residues in the cavity that contribute to the charge balance. To evaluate the importance in catalysis of residues His-67, Glu-87, and Arg-161, enzyme mutants H67N, E87Q, and R161Q were prepared and tested as described under "Experimental Procedures." The three mutant forms have been found to be unable to accelerate the spontaneous decay of OHCU (Fig. 3*D*), indicating that the replaced residues play a crucial role in catalysis or in maintaining the structural integrity of the active site.

The catalytic mechanism of decarboxylases in general implies the stabilization of the carbanion originating from decarboxylation, a task that can be achieved in several ways, often involving metal ions or cofactors or through delocalization into aromatic systems of the charge of the carbanion generated upon decarboxylation (29, 30). OHCU decarboxylase, however, does not employ cofactors or metal ions and the five-membered ring of the substrate is unable to delocalize the charge of the carbanion developing upon the release of CO_2. Therefore, a distinct catalytic mechanism of action is operating in OHCU decarboxylase. To postulate this mechanism, the non-enzymatic decarboxylation of OHCU, for which a mechanistic explanation implies the formation of an electrophilic center able to accept the electron pair donated upon the release of the carboxylate group, is taken into account; decarboxylation of carboxylic acids containing a C = N bond in β position is facilitated by protonation of the

FIGURE 3. **Amino acid residues involved in the interaction with substrate analogs and in catalytic activity.** *A*, stereo view of one of the enzyme active sites with bound (*R*)-allantoin. Electron density maps were calculated as omit maps and contoured at 3σ level. Possible H-bonds, corresponding to interatomic distances between atoms of bound ligand and protein atoms shorter than 3.1 Å, are shown as *dotted lines*. *B*, same as *panel A* for guanine. *C*, stereo view of the hypothetical OHCU-OHCU decarboxylase complex. One of the two possible stereoisomers of OHCU was modeled inside the active site in the position occupied by allantoin, without optimization. The only modification is a rotation of the His-67 side chain around its Cα-Cβ bond that brings it closer to the five-membered ring of the substrate. Distances are C5-NE His-67, 3.0 Å; OAE,OAD-OH Ser-84, 2.4 and 2.7 Å; OAE-NH3 Arg-161 3.1 Å; OAE-OE1 Glu-87, 2.9 Å. *D*, enzymatic activities of wild-type zebrafish OHCU decarboxylase and enzyme mutant forms were monitored by following the change of the OHCU-specific negative ellipticity at 257 nm by CD measurements (6). Upon rapid formation of OHCU, catalyzed by urate oxidase and HIU hydrolase, OHCU decarboxylation is revealed. Time courses in the absence of OHCU decarboxylase (*gray*) or in the presence of wild-type (*black*), H67N (*green*), E87Q (*light blue*), and R161Q (*dark blue*) OHCU decarboxylases are shown. The activity for the enzyme in which the non-catalytic 125 residue is replaced (L125M, *red*) is also shown. Reaction conditions: 1 unit of urate oxidase from *Candida utilis*, 2.5 μg of zebrafish HIU hydrolase, and 0.6 μg of zebrafish OHCU decarboxylase in a solution (1 ml) containing 0.1 mM urate and 0.1 M potassium phosphate buffer, pH 7.6; 22 °C.
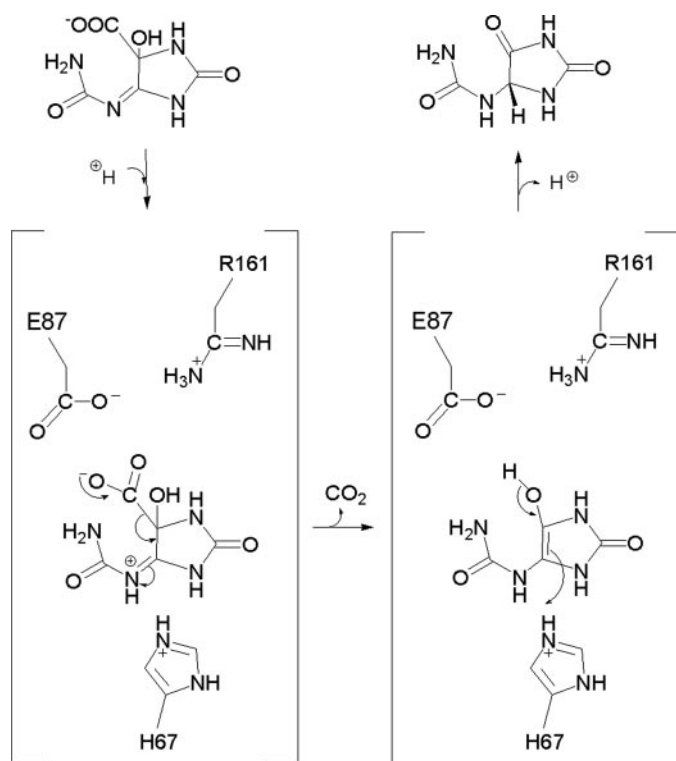
SCHEME 2. **The proposed mechanism of OHCU decarboxylation by OHCU decarboxylase.**

nitrogen atom participating in this bond to generate an effective electron sink (31). We thus propose that an initial step of the enzymatic decarboxylation of OHCU is the protonation of the substrate, afforded by a H_3O^+ molecule or by a protonated residue, resulting in the formation of an electron sink at N6 and allowing the release of CO_2 through an enol intermediate (Scheme 2). The proximity of the carboxylate group of Glu-87 could produce a destabilization of the ground state of the substrate, facilitating the release of its carboxylate group as CO_2. The deletion of a positive charge at position 161 also abolishes any activity. The charged side chain of Arg-161 directly interacts with Glu-87 and is at ~5 Å distance from the carboxylate group of the substrate. In this respect, the mechanism of action of OHCU decarboxylase is reminiscent of that of orotidine 5′-monophosphate decarboxylase, for which metal ions or cofactors are not required for catalysis: a network of four alternating charges has been revealed at the active site, and an electrostatic repulsion between the carboxylate groups of the substrate and of the side chain of an Asp residue present in the network possibly takes place (32, 33).

After the release of CO_2, an enol intermediate is formed, which rearranges to give the final keto product. The rearrangement of the enol intermediate, which in itself might take place without the assistance of the enzyme according to an enol-keto tautomerization, can be remarkably affected by the presence of His-67. This residue, which is likely to be protonated and is close enough to C5 atom of the substrate, can donate a proton to the enol intermediate to form the final keto product. Because His-67 is in the *re* position with respect to the mean plane of bound substrate, allantoin would be generated in the correct (*S*)

configuration. In this hypothesis, His-67 plays a major role in catalysis, acting as proton donor in the reaction and controlling its stereochemistry.

Structural data, coupled with site-directed mutagenesis experiments, have provided indications about the mechanism of action of OHCU decarboxylase. In particular, they strengthen the role of His-67 as proton donor and offer an explanation for the formation of the (*S*)-enantiomer of allantoin as reaction product.

REFERENCES

1. Vogels, G. D., and van der Drift, C. (1976) *Bacteriol. Rev.* **40,** 403–468
2. Modric, N., Derome, A. E., Ashcroft, S. J. H., and Poje, M. (1992) *Tetrahedron Lett.* **33,** 6691–6694
3. Khan, K., and Tipton, P. A. (1997) *Biochemistry* **36,** 4731–4738
4. Sarma, A. D., Serfozo, P., Khan, K., and Tipton, P. A. (1999) *J. Biol. Chem.* **274,** 33864–33865
5. Lee, Y., Lee, do H., Kho, C. W., Lee, A. Y., Jang, M., Cho, S., Lee, C. H., Lee, J. S., Myung, P. K., Park, B. C., and Park, S. G. (2005) *FEBS Lett.* **579,** 4769–4774
6. Ramazzina, I., Folli, C., Secchi, A., Berni, R., and Percudani, R. (2006) *Nat. Chem. Biol.* **2,** 144–148
7. Kahn, K., Serfozo, P., and Tipton, P. A. (1997) *J. Am. Chem. Soc.* **119,** 5435–5442
8. Lee, S. J., and Terkeltaub, R. A. (2006) *Curr. Rheumatol. Rep.* **8,** 224–230
9. Colloc'h, N., El Hajji, M., Bachet, B., L'Hermite, G., Schiltz, M., Prange, T., Castro, B., and Mornon, J. P. (1997) *Nat. Struct. Biol.* **4,** 947–952
10. Gabison, L., Chiadmi, M., Colloc'h, N., Castro, B., and El Hajji, M. (2006) *FEBS Lett.* **580,** 2087–2091
11. Colloc'h, N., Poupon, A., and Mornon, J. P. (2000) *Proteins* **39,** 142–154
12. Hennebry, S. C., Law, R. H., Richardson, S. J., Buckle, A. M., and Whisstock, J. C. (2006) *J. Mol. Biol.* **359,** 1389–1399
13. Jung, D. K., Lee, Y., Park, S. G., Park, B. C., Kim, G. H., and Rhee, S. (2006) *Proc. Natl. Acad. Sci. U. S. A.* **103,** 9790–9795
14. Lundberg, E., Backstrom, S., Sauer, U. H., and Sauer-Eriksson, A. E. (2006) *J. Struct. Biol.* **155,** 445–457
15. Zanotti, G., Cendron, L., Ramazzina, I., Folli, C., Percudani, R., and Berni, R. (2006) *J. Mol. Biol.* **363,** 1–9
16. Doublie, S. (1997) *Methods Enzymol.* **276,** 523–530
17. Matthews, B. (1968) *J. Mol. Biol.* **33,** 491–497
18. Collaborative Computing Project 4 (1994) *Acta Crystallogr. Sect. D. Biol. Crystallogr.* **50,** 760–763
19. Schneider, T. R., and Sheldrick, G. M. (2002) *Acta Crystallogr. Sect. D. Biol. Crystallogr.* **58,** 1772–1779
20. Bricogne, G., Vonrhein, C., Flensburg, M., Schiltz, M., and Paciorek, W. (2003) *Acta Crystallogr. Sect. D. Biol. Crystallogr.* **59,** 2023–2030
21. Emsley, P., and Cowtan, K. (2004) *Acta Crystallogr. Sect. D. Biol. Crystallogr.* **60,** 2126–2132
22. Brünger, A. T., Adams, P. D., Clore, G. M., DeLano, W. L., Gros, P., Grosse Kunstleve, R. W., Jiang, J. S., Kuszewski, J., Nilges, M., Pannu, N. S., Read, R. J., Rice, L. M., Simonson, T., and Warren, G. L. (1998) *Acta Crystallogr. Sect. D. Biol. Crystallogr.* **54,** 905–921
23. Murshudov, G. N., Vagin, A. A., and Dodson, E. J. (1997) *Acta Crystallogr. Sect. D. Biol. Crystallogr.* **53,** 240–255
24. Laskowski, R. A., MacArthur, M. W., Moss, D. S., and Thornton, J. M. (1993) *J. Appl. Crystallogr.* **26,** 283–291
25. Schuettelkopf, A. W., and van Aalten, D. M. F. (2004) *Acta Crystallogr.*

Sect. D. Biol. Crystallogr. **60,** 1355–1363

26. Laskowski, R. A., Watson, J. D., and Thornton, J. M. (2005) *Nucleic Acids Res.* **33,** W89–W93
27. Holm, L., and Sander, C. (1993) *J. Mol. Biol.* **233,** 123–138
28. DeLano, W. L. (2002) The PyMOL Molecular Graphics System, DeLano Scientific, San Carlos, CA
29. O'Leary, M. H. (1992) in *Enzymes* (Sigman, D. S., ed.) Vol. 20, pp. 235–269,

Academic, San Diego, CA

30. Begly, T. P., and Ealick, S. E. (2004) *Curr. Opin. Chem. Biol.* **8,** 508–515
31. Jencks, W. P. (1987) *Catalysis in Chemistry and Enzymology*, pp. 116–120, Dover Publication, New York
32. Wu, N., Mo, Y., Gao, J., and Pai, E. F. (2000) *Proc. Natl. Acad. Sci. U. S. A.* **97,** 2017–2022
33. Miller, B. G., and Wolfenden, R. (2002) *Annu. Rev. Biochem.* **71,** 847–885